Phase conjugation using the surface nonlinearity of a dense potassium vapor

Jeffery J. Maki, William V. Davis,* and Robert W. Boyd
The Institute of Optics, University of Rochester, Rochester, New York 14627

J. E. Sipe
Department of Physics, University of Toronto, Toronto, Ontario, Canada M5S 1A7
(Received 4 May 1992)

We observe optical phase conjugation using the surface nonlinearity of a dense atomic potassium vapor. For an atomic number density of 1.5×10^{17} cm^{-3}, phase-conjugate reflectivities of 4×10^{-5} are measured for pump intensities approaching the saturation intensity of 10 W cm^{-2}. We also demonstrate aberration correction using surface phase conjugation. The measured properties of the surface-phase-conjugate signal are in excellent agreement with the predictions of a theory of surface phase conjugation by degenerate four-wave mixing, in which the origin of the nonlinear response is saturated absorption.

PACS number(s): 42.65.Hw, 42.65.An, 32.70.Jz

I. INTRODUCTION

Surface phase conjugation [1] is a useful technique for achieving wave-front reversal by the nonlinear interaction of light with the surface of a material. Only two applied beams are required. A pump beam is applied at normal incidence and a probe beam (to be phase conjugated) is applied at an oblique angle of incidence (see Fig. 1). The nature of the nonlinear response is that the surface reflectivity changes with the intensity of the total incident optical field. Thus the interference of the pump and probe waves forms a spatially varying reflectivity pattern across the surface that scatters pump light to form the phase-conjugate (PC) wave.

Surface phase conjugation has been observed using many different materials. A surface-phase-conjugate (SPC) signal can result from optical damage of a metal mirror [2,3], deformation of a surface due to thermal expansion following the absorption of the incident radiation [4,5], modification of the optical properties of a surface layer due to plasma generation in a semiconductor [6,7], changes in the optical properties of a material due to a thermally induced phase transition [8], or the nonlinear response of an atomic vapor [9]. In related experiments, optical phase conjugation has been demonstrated by using a liquid-crystal light value that responds to the total incident optical field [10] and by using geometries where the applied waves are strongly coupled to electromagnetic surface waves [11,12]. Surface phase conjugation was first proposed in the theoretical paper by Zel'dovich *et al.* [13], which contains a general treatment of the process. Additional theoretical treatments have been developed, but they are specialized to cases of four-wave mixing of electromagnetic surface waves [14,15] using geometries different from that shown in Fig. 1.

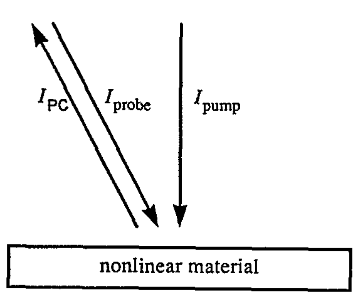

FIG. 1. Typical geometry of surface phase conjugation.

In this paper, we develop a quantitative theory of surface phase conjugation, using the geometry shown in Fig. 1, for materials possessing a third-order nonlinear-optical response. For these materials, the generation of the SPC wave is due to degenerate four-wave mixing (DFWM). We derive explicit formulas for the SPC reflectivity and compare these predictions with the results of our experiments.

We observe surface phase conjugation by DFWM using the interface between a potassium vapor and the flat window of the cell that contains the vapor. We also demonstrate experimentally that a SPC mirror can be used to correct for aberrations.

This paper is organized as follows. In Sec. II, we recall the general result of Ref. [16] for the electric field generated by the nonlinear polarization of the linear-nonlinear interface. The SPC reflectivity is calculated in Sec. III using the result of Sec. II. We complete the theoretical development of this paper by briefly reviewing in Sec. IV the optical properties of a dense atomic vapor. The results of our experimental study are given in Sec. V, and finally the conclusions of this work are given in Sec. VI.

II. NONLINEAR POLARIZATION AND THE GENERATED ELECTRIC FIELD

In linear optics, a plane wave that is incident upon a flat surface (the x-y plane) formed by the boundary between two homogeneous materials breaks up into a transmitted wave and a specularly reflected wave that obeys the *law of reflection.* The superposition principle may then be used to analyze the transmission and reflection of an arbitrary wave front consisting of many different plane waves. In nonlinear optics, the interaction of intense light with a material may lead to spatial inhomogeneity of the index of refraction of the material, even though in the linear regime the material possesses a homogeneous index of refraction. This inhomogeneity results from the nonlinear polarization driven by the incident electric field. The nonlinear polarization need not have the same component of its wave vector in the x-y plane as that of the incident electric field. Hence, the portion of the nonlinear polarization with the same wave-vector component as the incident electric field leads to a modification of the Fresnel reflection coefficient, and the portion with a wave-vector component opposite in sign to that of the incident electric field leads to the process of surface phase conjugation.

In this section, we give a brief review of the relation between the nonlinear polarization and the electric field that is generated [16]. We deal throughout with monochromatic fields of the form

$$\mathbf{F}(\mathbf{r},t)=\mathbf{F}(\mathbf{r})e^{-i\omega t}+\text{c.c.} \tag{1}$$

Suppose that a nonlinear polarization of the form

$$\mathbf{P}(\mathbf{r})=\tilde{\mathbf{P}}(z)\exp(i\boldsymbol{\kappa}\cdot\mathbf{R}) \tag{2}$$

is induced in the medium m (i.e., $z<0$), where $\mathbf{r}=z\hat{\mathbf{z}}+\mathbf{R}$ and $\mathbf{R}=x\hat{\mathbf{x}}+y\hat{\mathbf{y}}$, and where $\hat{\mathbf{x}}$, $\hat{\mathbf{y}}$, and $\hat{\mathbf{z}}$ are the Cartesian unit vectors (see Fig. 2). The nonlinear polarization has been assumed to have a component $\boldsymbol{\kappa}=\kappa\hat{\boldsymbol{\kappa}}$ of its wave vector that is transverse to the surface, but at this stage we allow the z dependence of the nonlinear polarization to be completely arbitrary. An electric field

$$\mathbf{E}(\mathbf{r})=\tilde{\mathbf{E}}(z)\exp(i\boldsymbol{\kappa}\cdot\mathbf{R}) \tag{3}$$

will be generated by this nonlinear polarization [Eq. (2)] that propagates with the same wave-vector component $\boldsymbol{\kappa}$.

The portion of the electric field generated by the nonlinear polarization that is transmitted into the material g (i.e., $z>0$) can be written in the form

$$\mathbf{E}(\mathbf{r})=\mathbf{E}_0\exp(i\mathbf{k}_{g+}\cdot\mathbf{r})\ , \tag{4}$$

where the wave vector of propagation in the material g is $\mathbf{k}_{g+}=\kappa\hat{\boldsymbol{\kappa}}+w_g\hat{\mathbf{z}}$, $w_g=(\tilde{\omega}^2n_g^2-\kappa^2)^{1/2}$, $\tilde{\omega}=\omega/c$, and n_g is the linear index of refraction of material g. The electric

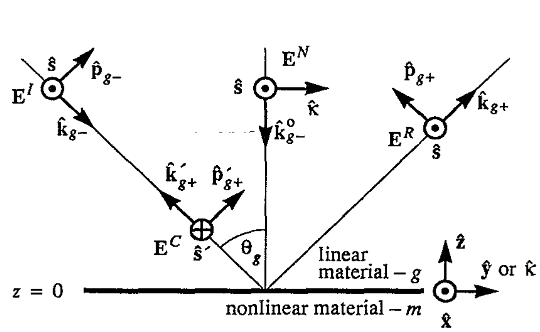

FIG. 2. Unit vectors for the applied and generated waves of surface phase conjugation and nonlinear Fresnel reflection. The *circles* with dots or crosses indicate vectors out of or into the drawing, respectively.

field amplitude $\mathbf{E}_0$ of Eq. (4) is shown in Ref. [16] to be

$$\mathbf{E}_0=i2\pi\tilde{\omega}^2w_m^{-1}(\hat{\mathbf{s}}t^s_{mg}\hat{\mathbf{s}}+\hat{\mathbf{p}}_{g+}t^p_{mg}\hat{\mathbf{p}}_{m+})\cdot\int_{-\infty}^{0}\exp(-iw_mz')\times\tilde{\mathbf{P}}(z')dz'\ . \tag{5}$$

The linear Fresnel amplitude transmission coefficients [17] t^s_{mg} and t^p_{mg} for s- and p-polarized radiation describe the transmission of radiation generated in the material m into the material g. The quantity $w_m=(\tilde{\omega}^2n_m^2-\kappa^2)^{1/2}$ is the longitudinal component (perpendicular to the x-y plane) of the wave vector of light that propagates in the material m, where n_m is the linear index of refraction of medium m. For the generated light that propagates in the positive z direction, the s and p polarizations of the generated light are specified by the unit vectors $\hat{\mathbf{s}}\equiv\hat{\boldsymbol{\kappa}}\times\hat{\mathbf{z}}$ and $\hat{\mathbf{p}}_{m+}=(\kappa\hat{\mathbf{z}}-w_m\hat{\boldsymbol{\kappa}})/(\tilde{\omega}n_m)$ in medium m, and $\hat{\mathbf{s}}$ and $\hat{\mathbf{p}}_{g+}=(\kappa\hat{\mathbf{z}}-w_g\hat{\boldsymbol{\kappa}})/(\tilde{\omega}n_g)$ in medium g.

III. THEORY OF SURFACE PHASE CONJUGATION

In the previous section, an expression [Eq. (5)] was given for the electric field generated by an arbitrary nonlinear polarization. In this section, an approximate expression for the nonlinear polarization leading to the generation of a SPC wave is specified in detail. Using this expression for the nonlinear polarization, we derive analytic expressions for the SPC electric field and intensity reflectivity.

Consider the incident waves ($z>0$) as depicted in Fig. 2. The electric field of the probe wave is

$$\mathbf{E}^I(\mathbf{r})=\tilde{\mathbf{E}}^I(z)\exp(i\boldsymbol{\kappa}\cdot\mathbf{R})\ , \tag{6}$$

where $\kappa=\tilde{\omega}n_g\sin\theta_g$ and θ_g is the angle of incidence, and

$$\tilde{\mathbf{E}}^I(z)=[\hat{\mathbf{s}}E^I_s+\hat{\mathbf{p}}_{g-}E^I_p]\exp(-i\omega_gz)\ . \tag{7}$$

The electric field of the normally incident pump wave is

$$\mathbf{E}^N(\mathbf{r})=\tilde{\mathbf{E}}^N(z)=[\hat{\mathbf{s}}E^N_s+\hat{\boldsymbol{\kappa}}E^N_p]\exp(-i\tilde{\omega}n_gz)\ . \tag{8}$$

Note that the pump wave does not have a component of its wave vector that is in the x-y plane; and the field amplitudes E^I_s, E^I_p, E^N_s, and E^N_p are all assumed to be constant. The total incident optical field is given by the sum $\mathbf{E}_{\text{inc}}(\mathbf{r})=\tilde{\mathbf{E}}^I(z)\exp(i\boldsymbol{\kappa}\cdot\mathbf{R})+\tilde{\mathbf{E}}^N(z)$ of the electric fields of the probe and pump waves in the linear optical material g.

We assume that the nonlinearity is sufficiently weak that the incident electric field transmitted into the nonlinear material m (i.e., $z<0$) is given by the sum

$$\mathbf{E}_{\text{tran}}(\mathbf{r})=\tilde{\mathbf{E}}^I(z)\exp(i\boldsymbol{\kappa}\cdot\mathbf{R})+\tilde{\mathbf{E}}^N(z)\ , \tag{9a}$$

where

$$\tilde{\mathbf{E}}^I(z)=[\hat{\mathbf{s}}t^s_{gm}E^I_s+\hat{\mathbf{p}}_{m-}t^p_{gm}E^I_p]\exp(-iw_mz)\ , \tag{9b}$$

$$\tilde{\mathbf{E}}^N(z)=[\hat{\mathbf{s}}t^0_{gm}E^N_s+\hat{\boldsymbol{\kappa}}t^0_{gm}E^N_p]\exp(-i\tilde{\omega}n_mz)\ . \tag{9c}$$

The transmission of the incident light into the material m is treated through the use of the linear Fresnel amplitude transmission coefficients [17] t_{gm}^s and t_{gm}^p for the s- and p-polarized components to the probe wave and t_{gm}^0 for the pump wave. The unit vectors for the p polarization of the incident and transmitted light are $\hat{\mathbf{p}}_{g-}=(\kappa\hat{\mathbf{z}}+w_g\hat{\boldsymbol{\kappa}})/(\tilde{\omega}n_g)$ and $\hat{\mathbf{p}}_{m-}=(\kappa\hat{\mathbf{z}}+w_m\hat{\boldsymbol{\kappa}})/(\tilde{\omega}n_m)$, respectively [16].

The nonlinearity of a centrosymmetric material may be treated by the Maker-Terhune [18] expression for the third-order nonlinear polarization

$$\mathbf{P}(\mathbf{r})=A[\mathbf{E}_{\rm tot}(\mathbf{r})\cdot\mathbf{E}_{\rm tot}^*(\mathbf{r})]\mathbf{E}_{\rm tot}(\mathbf{r}) + \tfrac{1}{2}B[\mathbf{E}_{\rm tot}(\mathbf{r})\cdot\mathbf{E}_{\rm tot}(\mathbf{r})]\mathbf{E}_{\rm tot}^*(\mathbf{r}) \,, \tag{10}$$

where A and B are tensor components of the third-order susceptibility [19] with $\mathbf{E}_{\rm tot}(\mathbf{r})$ is the total electric field. Consistent with the assumption that the nonlinearity is weak, the electric field that drives the nonlinear polarization is taken to be the transmitted electric field [Eq. (9)]. Thus, using $\mathbf{E}_{\rm tot}\cong\mathbf{E}_{\rm tran}$ in Eq. (10) and expanding that equation, many terms result, of which two have a wave-vector component (i.e., in the x-y plane) to form a PC wave. Hence, the polarization for the PC wave is $\mathbf{P}^C(\mathbf{r})=\tilde{\mathbf{P}}^C(z)\exp(i\boldsymbol{\kappa}'\cdot\mathbf{R})$, where $\boldsymbol{\kappa}'=-\boldsymbol{\kappa}$, and

$$\tilde{\mathbf{P}}^C(z)=A[\tilde{\mathbf{E}}^N(z)\cdot\tilde{\mathbf{E}}^{I*}(z)]\tilde{\mathbf{E}}^N(z) + \tfrac{1}{2}B[\tilde{\mathbf{E}}^N(z)\cdot\tilde{\mathbf{E}}^N(z)]\tilde{\mathbf{E}}^{I*}(z) \,. \tag{11}$$

Consider the cases in which the pump and probe waves are both s polarized or are both p polarized. (More general cases could be considered, but they would unduly complicate the following discussion). The conjugate-wave polarization [Eq. (11)] is

$$\tilde{\mathbf{P}}_s^C(z)=\hat{\mathbf{s}}(A+\tfrac{1}{2}B)t_{gm}^0 t_{gm}^0 t_{gm}^{s*}E_s^N E_s^N E_s^{I*} \times\exp[i(w_m^*-2\tilde{\omega}n_m)z] \tag{12}$$

for the case of s-polarized light and

$$\tilde{\mathbf{P}}_p^C(z)=\left[\hat{\boldsymbol{\kappa}}A\frac{w_m^*}{\tilde{\omega}n_m^*}+\hat{\mathbf{p}}_{m-}^*\tfrac{1}{2}B\right]t_{gm}^0 t_{gm}^0 t_{gm}^{p*}E_p^N E_p^N E_p^{I*} \times\exp[i(w_m^*-2\tilde{\omega}n_m)z] \tag{13}$$

for the case of p-polarized light.

The electric field of the SPC wave (see Fig. 2) is

$$\mathbf{E}^C(\mathbf{r})=\mathbf{E}_0^C\exp(i\mathbf{k}_{g+}'\cdot\mathbf{r}) \,, \tag{14}$$

where $\mathbf{k}_{g+}'=\kappa\hat{\boldsymbol{\kappa}}'+w_g\hat{\mathbf{z}}$. Using Eq. (5), the amplitude $\mathbf{E}_0^C$ of the SPC wave is given by

$$\mathbf{E}_0^C=i2\pi\tilde{\omega}^2w_m^{-1} \times(\hat{\mathbf{s}}'t_{mg}^s\hat{\mathbf{s}}'+\hat{\mathbf{p}}_{g+}'t_{mg}^p\hat{\mathbf{p}}_{m+}')\cdot\int_{-\infty}^0\exp(-iw_mz') \times\tilde{\mathbf{P}}^C(z')dz' \,, \tag{15}$$

where $\hat{\mathbf{s}}'\equiv\hat{\boldsymbol{\kappa}}'\times\hat{\mathbf{z}}$, $\hat{\mathbf{p}}_{g+}'=(\kappa\hat{\mathbf{z}}-w_g\hat{\boldsymbol{\kappa}}')/(\tilde{\omega}n_g)$, and $\hat{\mathbf{p}}_{m+}'=(\kappa\hat{\mathbf{z}}-w_m\hat{\boldsymbol{\kappa}}')/(\tilde{\omega}n_m)$. Thus, using expressions [Eqs. (12) and (13)] for the conjugate polarization, the amplitude $\mathbf{E}_0^C$ is given by

$$\mathbf{E}_s^C=\hat{\mathbf{s}}'(A+\tfrac{1}{2}B)\frac{\pi\tilde{\omega}^2w_m^{-1}}{[\tilde{\omega}n_m+i\,{\rm Im}(w_m)]}t_{mg}^s t_{gm}^0 t_{gm}^0 t_{gm}^{s*}E_s^N E_s^N E_s^{I*} \tag{16}$$

for s-polarized light and

$$\mathbf{E}_p^C=-\hat{\mathbf{p}}_{g+}'\left[A\left|\frac{w_m}{n_m}\right|^2+\tfrac{1}{2}B\frac{(|\kappa|^2+|w_m|^2)}{|n_m|^2}\right] \times\frac{\pi w_m^{-1}}{[\tilde{\omega}n_m+i\,{\rm Im}(w_m)]}t_{mg}^p t_{gm}^0 t_{gm}^0 t_{gm}^{p*}E_p^N E_p^N E_p^{I*} \tag{17}$$

for p-polarized light.

The intensity reflectivity for the SPC mirror is defined by $R^{\rm PC}\equiv|\mathbf{E}_0^C|^2/|\mathbf{E}_0^I|^2$. For s-polarized light, the SPC intensity reflectivity is

$$R_s^{\rm PC}=\frac{4\pi^4|A+\tfrac{1}{2}B|^2}{c^2\epsilon_g|n_m\cos\theta_m|^2|n_m+i\,{\rm Im}(n_m\cos\theta_m)|^2} \times|t_{gm}^s|^2|t_{mg}^s|^2|t_{gm}^0|^4I_{\rm pump}^2 \,, \tag{18}$$

and for p-polarized light, the SPC intensity reflectivity is

$$R_p^{\rm PC}=\frac{4\pi^4|A|\cos\theta_m|^2+\tfrac{1}{2}B(|\sin\theta_m|^2+|\cos\theta_m|^2)|^2}{c^2\epsilon_g|n_m\cos\theta_m|^2|n_m+i\,{\rm Im}(n_m\cos\theta_m)|^2} \times|t_{gm}^p|^2|t_{mg}^p|^2|t_{gm}^0|^4I_{\rm pump}^2 \,, \tag{19}$$

where the intensity of the pump wave in the material g is given by $I_{\rm pump}=(cn_g/2\pi)|\mathbf{E}^N|^2$, $\cos\theta_m=w_m/(\tilde{\omega}n_m)$, $\epsilon_g=n_g^2$, and $\epsilon_m=n_m^2$.

The Fresnel reflection $\mathbf{E}^R$ (see Fig. 2) of the probe wave $\mathbf{E}^I$ will also be modified due to contributions from the nonlinear polarization [Eq. (10)]. The contributions are driven by the probe wave itself and by the presence of both the probe and pump waves. We have included in the Appendix a brief derivation of the nonlinear Fresnel reflectivities.

IV. OPTICAL RESPONSE OF AN ATOMIC POTASSIUM VAPOR

The origin of the nonlinear-optical response of atomic potassium is the saturable absorption of light for frequencies near a resonance frequency. The key resonances of potassium are the $4\,^2S_{1/2}\leftrightarrow4\,^2P_{1/2}$ and $4\,^2S_{1/2}\leftrightarrow4\,^2P_{3/2}$ atomic transitions, which have a vacuum transition wavelength λ_0 of 770.1 and 766.7 nm, respectively. The description of the linear and third-order nonlinear-optical response of an atomic potassium vapor follows from Ref. [20].

The linear dielectric constant ϵ_m of a vapor with atomic number density N is given by

$$\epsilon_m=1+\frac{fr_e\lambda_0cN}{\omega_0+\Delta\omega_{\rm col}+\Delta\omega_L-\omega-i\gamma_2} \,, \tag{20}$$

where f is the absorption oscillator strength, $r_e=e^2/(mc^2)$ is the classical electron radius, $\omega_0=2\pi c/\lambda_0$ is the transition frequency, $\Delta\omega_{\rm col}$ is the shift of the atomic resonance due to collisions between potassium atoms,

$\Delta\omega_L = -\frac{1}{3} f r_e \lambda_0 c N$ is the Lorentz redshift of a dense atomic vapor, and γ_2 is the half-width at half maximum (HWHM) linewidth. The Lorentz redshift is a consequence of local-field effects [21,22], and was recently studied by ourselves within the context of surface phase conjugation [20].

The scalar third-order susceptibility [actually, $\chi^{(3)} \equiv \chi^{(3)}_{1111} = \frac{1}{3}(A + B/2)$] of a dense vapor is given by

$$\chi^{(3)} = L^2 |L|^2 \frac{f r_e \lambda_0 c N}{12\pi\gamma_2 |E^0_{\text{sat}}|^2} \frac{(\delta - i)}{(1+\delta^2)^2} , \tag{21}$$

where the Lorentz local-field correction factor is $L = (\epsilon_m + 2)/3$, the normalized detuning from resonance is $\delta = (\omega - \omega_0 - \Delta\omega_{\text{col}})/\gamma_2$, the saturation parameter for the atomic resonance is

$$|E^0_{\text{sat}}|^2 = \frac{\gamma_{\text{nat}} \gamma_2 h}{2 f r_e \lambda_0 c} , \tag{22}$$

and h is the Planck constant.

The HWHM atomic linewidth is the sum $\gamma_2 = \frac{1}{2}\gamma_{\text{nat}} + \gamma_{\text{self}}$ of the contributions from natural broadening γ_{nat} and from self-broadening [23]

$$\gamma_{\text{self}} = \left[\frac{2J_g + 1}{2J_e + 1} \right]^{1/2} f r_e \lambda_0 c N , \tag{23}$$

where J_g and J_e are the angular momentum quantum numbers of the ground and excited states, respectively. For potassium [24], the spontaneous emission population decay rate is $\gamma_{\text{nat}} = 4.0 \times 10^7\ \text{sec}^{-1}$.

The shift of the atomic transition resonance frequency is found empirically to increase linearly with the atomic number density according to $\Delta\omega_{\text{col}} = \beta N$. The measured value of β is given in Ref. [20] to be $-5.0 \times 10^{-8}\ \text{sec}^{-1}\ \text{cm}^3$ for the $4\,^2S_{1/2} \leftrightarrow 4\,^2P_{1/2}$ transition ($f = 0.339$) and $-3.0 \times 10^{-8}\ \text{sec}^{-1}\ \text{cm}^3$ for the $4\,^2S_{1/2} \leftrightarrow 4\,^2P_{3/2}$ transition ($f = 0.682$). The values of the absorption oscillator strength f are taken from Ref. [24].

The linear- and nonlinear-optical response of a potassium vapor depends on the atomic number density N in a complicated manner due to the dependence of the linewidth γ_2 and shift $\Delta\omega_{\text{col}}$ upon N. For instance, the on-resonance saturation intensity $I^0_{\text{sat}} = (c/2\pi)|E^0_{\text{sat}}|^2$ depends directly upon γ_2 [see Eq. (22)], and hence increases with increasing values of the number density N. Nonetheless, the optical response can be enhanced by using a vapor with a large value of the number density N.

V. EXPERIMENT

We investigate surface phase conjugation using an atomic vapor because an accurate description of the linear and nonlinear optical response is possible. Furthermore, for temperatures of a potassium vapor in excess of 430 °C, the atomic number density can be in excess of $10^{17}\ \text{cm}^{-3}$, which results in a penetration depth into the vapor of approximately $\lambda/2\pi$ for resonant light. Thus, as a saturable absorber, at atomic potassium vapor can be used to form a material possessing a surface nonlinearity.

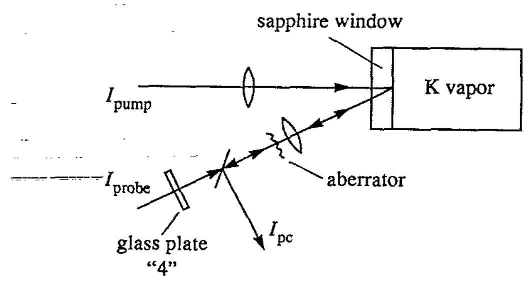

FIG. 3. Schematic of the experimental setup used to demonstrate aberration correction and to measure the SPC signal (without the aberrator and glass plate).

The experimental setup used to study surface phase conjugation is shown in Fig. 3. A pump beam I_{pump} is incident upon a vapor cell such that it is normal to the interface between the vapor and the sapphire plate that forms the window of the cell. The probe beam I_{probe} is incident at an oblique angle ($\theta_g = 14.4°$). The pump and probe waves are both s polarized, and the optic axis of the sapphire plate is aligned such that the pump and probe waves travel as ordinary waves ($n_g = 1.76$) within the sapphire. In addition, the pump and probe waves are weakly focused by lenses. The output of a Coherent 699-21 continuous-wave ring-dye laser is used to form the pump and probe beams. The laser operates with a 2–3 MHz bandwidth and can scan 30 GHz of the optical spectrum.

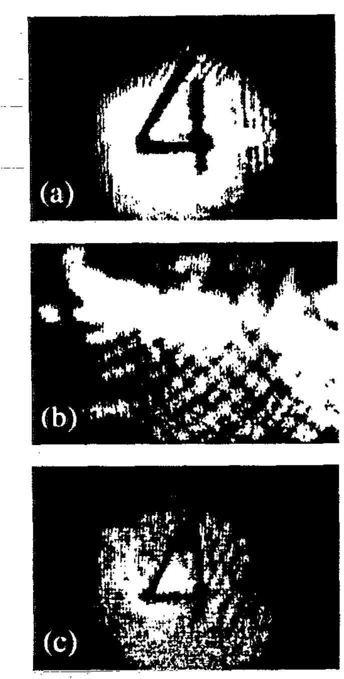

FIG. 4. (a) Image-bearing beam. (b) Image-bearing beam after retracting the aberrator due to reflection by an ordinary mirror. (c) Image-bearing beam after retracting the aberrator due to reflection by a SPC mirror. In (c), the wave-front reversal of the SPC mirror causes the aberration seen in (b) to be removed.

The interaction of the probe and the pump waves are observed to lead to the generation of a beam of light (labeled I_{PC} in Fig. 3) that propagates in a direction opposite to that of the incident probe beam. We determine whether this beam is the phase conjugate of the probe beam by conducting the standard test of aberration correction in double pass. In this test, the probe beam and the generated beam are made to counterpropagate through an aberrator (see Fig. 3). If the generated beam is the phase conjugate of the probe beam, then any wave-front distortions impressed upon the probe beam by the aberrator will be removed from the generated beam, after the generated beam has propagated through the aberrator. Our experimental results shown in Fig. 4 show that the wave-front distortions of the aberrator can be removed. Thus the generated beam is the phase conjugate of the probe beam.

Figure 5(a) shows some recordings of the SPC reflectivity as a function of the detuning of the laser frequency from the $4\,^2S_{1/2} \leftrightarrow 4\,^2P_{1/2}$ atomic resonance frequency. Each curve corresponds to a different value of the atomic number density, namely, 7.7×10^{16}, 9.0×10^{16}, 1.1×10^{17}, and 1.5×10^{17} cm^{-3}. The progression from small to large values of the number density is indicated by the arrow. With increasing values of the number density N, the peak value of the SPC reflectivity decreases due to the increase in the saturation intensity.

The corresponding theoretical predictions for the SPC reflectivity are shown in Fig. 5(b). These predictions are calculated using the formula for the SPC reflectivity of s-polarized light [Eq. (18)], which may be rewritten in the form

$$R_s^{PC} = \frac{36\pi^4|\chi^{(3)}|^2}{c^2\epsilon_g|n_m\cos\theta_m|^2|n_m+i\,\mathrm{Im}(n_m\cos\theta_m)|^2} \times |t_{gm}^2|^2|t_{mg}^s|^2|t_{gm}^0|^4 I_{\mathrm{pump}}^2 \qquad (24)$$

in order to show explicitly the dependence upon the scalar third-order susceptibility $\chi^{(3)}$. The transmission coefficients t_{gm}^s, t_{mg}^s, and t_{gm}^0 are calculated using the standard Fresnel formulas [17], where the index of refraction $n_m=\sqrt{\epsilon_m}$ of the atomic vapor is calculated using Eq. (20). The free parameter in making the comparison shown in Fig. 5 is the amplitude of the highest curve in both the experimental and theoretical family of curves. Figure 5 thus illustrates that the theory accounts for the dominate effects observed in the experiment, which are the variation of the SPC reflectivity with optical frequency ω and atomic number density N.

In Fig. 6, we further illustrate the agreement between the results of the experiment and the predictions of the theory by plotting the variation of the SPC reflectivity with optical frequency for a number density of 1.5×10^{17} cm^{-3}. The peak value of the SPC reflectivity is not centered on the single-atom resonance frequency ω_0, but is 2.2 GHz to the red side of resonance. There is an intrinsic frequency shift of the optical response due both to the collisions of potassium atoms (i.e., $\Delta\omega_{\mathrm{col}}$) and to the effects of Lorentz local-field corrections [20].

For the peak value of the SPC reflectivity in Fig. 6, the value of the third-order susceptibility $\chi^{(3)}$ is calculated to be $0.60-i1.2$ esu. The corresponding intensity-dependent refractive index n_2 can be defined through the relation $n_{\mathrm{tot}}=n_m+n_2I$ for the total index of refraction to third order, where the intensity is $I=(c/2\pi)|E|^2$. Hence the intensity-dependent refractive index is given by $n_2=(12\pi^2/cn_m)\chi^{(3)}$ and has the value of $2.0\times10^{-3}-i4.6\times10^{-2}$ cm^{2}W^{-1}, where we note that the linear index of refraction is $n_m=1.04+i0.47$.

The validity of the model of surface phase conjugation presented in this paper is limited to values of the intensity I that are much less than the saturation intensity $I_{\mathrm{sat}}=I_{\mathrm{sat}}^0(1+\delta^2)$. For instance, at the number density of 1.5×10^{17} cm^{-3}, the on-resonance saturation intensity I_{sat}^0 of the potassium vapor is 10 W cm^{-2}. In order to obtain the largest values of the SPC reflectivity, however, the intensity of the pump beam typically needs to be close to the saturation intensity. Even then, the largest value of the reflectivity is measured to be 4×10^{-5} for a number density of 1.5×10^{17} cm^{-3}.

We measure the SPC reflectivity over a range of number densities by varying the temperature of the cell. In Fig. 7, measurements of the full width at half maximum (FWHM) γ_{PC} of the SPC reflectivity are plotted as a function of the atomic number density ranging from 1.6×10^{16} to 1.5×10^{17} cm^{-3}. The corresponding theoretical prediction, shown by a straight line in Fig. 7, does not include effects of Doppler broadening. The Doppler-broadened (FWHM) linewidth of the linear response is predicted to be 1.2 GHz. As seen in Fig. 7, the predictions of the theory agree with the measured

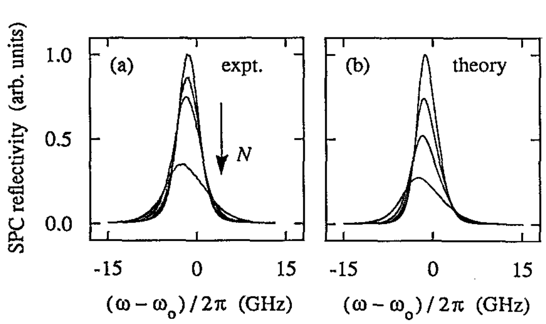

FIG. 5. SPC reflectivity plotted as a function of detuning from the $4\,^2S_{1/2} \leftrightarrow 4\,^2P_{1/2}$ atomic resonance frequency for various values of the atomic number density.

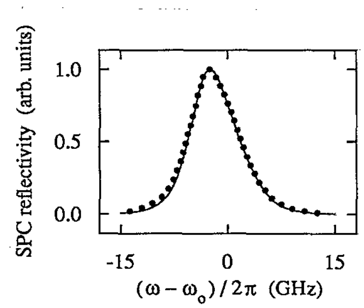

FIG. 6. SPC reflectivity from Fig. 5, for a number density of $N=1.5\times10^{17}$ cm^{-3}. The solid circles are the measured values and the line is the corresponding theoretical prediction.

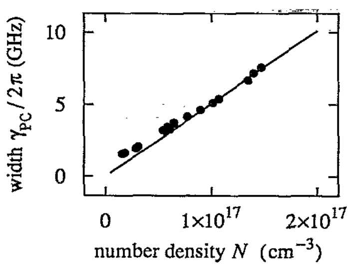

FIG. 7. Spectral width γ_{PC} (full width at half maximum) of the SPC reflectivity plotted as a function of the atomic number density for the $4\,^2S_{1/2}\leftrightarrow 4\,^2P_{1/2}$ atomic transition. The values measured in the experiment are given by the solid circles and the corresponding theoretical prediction is given by the straight line.

values of the SPC spectral width, but there is some disagreement for number density below 2.0×10^{16} cm^{-3}, where the width γ_{PC} is comparable to the Doppler width. For values of the number density well below 2.0×10^{16} cm^{-3}, Doppler broadening is the dominant line-broadening mechanism, the value of $\chi^{(3)}$ is greatly reduced, and no SPC signal appears.

VI. CONCLUSIONS

We have developed a detailed theory of surface phase conjugation for s- and p-polarized light. The theory is valid for any homogeneous material possessing a nonlinear response that can be described by a third-order susceptibility. We give explicit formulas for the SPC reflectivity and, in addition, we give formulas for the specular reflectivity including the contribution from nonlinear polarization.

We have observed surface phase conjugation using a dense atomic potassium vapor. The results of our measurements of the SPC reflectivity are in excellent agreement with the predictions of the theory of surface phase conjugation derived in this paper. The largest value of the SPC reflectivity observed is 4×10^{-5} for pump intensities approaching the saturation intensity of 10 W cm^{-2}. In addition, the potassium SPC mirror is shown to be capable of correcting for aberrations in double pass.

ACKNOWLEDGMENTS

We gratefully acknowledge the help of M. S. Malcuit. One of us (J.J.M.) would like to thank the Phillips Laboratory (formerly the Air Force Weapons Laboratory) for financial support.

APPENDIX: NONLINEAR FRESNEL REFLECTION

A probe wave $\mathbf{E}^I$ incident upon an interface between a linear and a nonlinear material will be specularly reflected $\mathbf{E}^R$ (see Fig. 2). This reflection will depend upon the nonlinear polarization that is induced in the material m. The third-order nonlinear polarization that contributes to specular reflection is found using Eq. (10) to be

$$\mathbf{P}^R(\mathbf{r})=[\tilde{\mathbf{P}}^{RS}(z)+\tilde{\mathbf{P}}^{RX}(z)]\exp(i\kappa\cdot\mathbf{R}) , \tag{A1a}$$

where

$$\tilde{\mathbf{P}}^{RS}(z)=A[\tilde{\mathbf{E}}^I(z)\cdot\tilde{\mathbf{E}}^{I*}(z)]\tilde{\mathbf{E}}^I(z)+\tfrac{1}{2}B[\tilde{\mathbf{E}}^I(z)\cdot\tilde{\mathbf{E}}^I(z)]\tilde{\mathbf{E}}^{I*}(z) , \tag{A1b}$$

$$\tilde{\mathbf{P}}^{RX}(z)=A[\tilde{\mathbf{E}}^I(z)\cdot\tilde{\mathbf{E}}^{N*}(z)]\tilde{\mathbf{E}}^N(z)+A[\tilde{\mathbf{E}}^N(z)\cdot\tilde{\mathbf{E}}^{N*}(z)]\tilde{\mathbf{E}}^I(z)+B[\tilde{\mathbf{E}}^N(z)\cdot\tilde{\mathbf{E}}^I(z)]\tilde{\mathbf{E}}^{N*}(z) . \tag{A1c}$$

Note that the amplitude $\tilde{\mathbf{P}}^{RS}(z)$ depends only upon the presence of the probe wave and the amplitude $\tilde{\mathbf{P}}^{RX}(z)$ depends upon the presence of both the probe and pump waves.

The contributions to the Fresnel reflection of the probe wave from nonlinear-wave mixing are found by using Eq. (5) directly, where Eq. (9b) is used for the probe amplitudes $\tilde{\mathbf{E}}^I(z)$ and Eq. (9c) is used for the pump amplitude $\tilde{\mathbf{E}}^N(z)$. In addition to the contributions from nonlinear-wave mixing, the contribution from the process of linear Fresnel reflection must be included in order to find the total electric field that is specularly reflected. The specularly reflected wave may be written in the form $\mathbf{E}^R(\mathbf{r})=\mathbf{E}_0^R\exp(i\mathbf{k}_{g+}\cdot\mathbf{r})$, where $\mathbf{k}_{g+}=\kappa\hat{\kappa}+w_g\hat{\mathbf{z}}$. For s-polarized light, the electric-field amplitude is $\mathbf{E}_0^R=\hat{\mathbf{s}}r_{gm}^s E_s^I+\mathbf{E}_s^{RS}+\mathbf{E}_s^{RX}$, where r_{gm}^s is the linear Fresnel amplitude reflectivity [17] and the nonlinear contributions are given by

$$\mathbf{E}_s^{RS}=-\hat{\mathbf{s}}\frac{\pi\bar{\omega}^2 w_m^{-1}(A+\frac{1}{2}B)}{[w_m+i\,\mathrm{Im}(w_m)]}t_{mg}^s t_{gm}^s E_s^I|t_{gm}^s E_s^I|^2 , \tag{A2a}$$

$$\mathbf{E}_s^{RX}=-\hat{\mathbf{s}}\frac{2\pi\bar{\omega}^2 w_m^{-1}(A+\frac{1}{2}B)}{[w_m+i\bar{\omega}\,\mathrm{Im}(n_m)]}t_{mg}^s t_{gm}^s E_s^I|t_{gm}^0 E_s^N|^2 . \tag{A2b}$$

For p-polarized light, the electric-field amplitude is $\mathbf{E}_0^R=\hat{\mathbf{p}}_{g+}r_{gm}^p E_p^I+\mathbf{E}_p^{RS}+\mathbf{E}_p^{RX}$, where r_{gm}^p is the linear Fresnel amplitude reflectivity and the nonlinear contributions are given by

$$\mathbf{E}_p^{RS}=-\hat{\mathbf{p}}_{g+}\left[A\left[\frac{\kappa^2-w_m^2}{\bar{\omega}^2\epsilon_m}\right]\left[\frac{|\kappa|^2+|w_m|^2}{\bar{\omega}^2|n_m|^2}\right]+\tfrac{1}{2}B\left[\frac{|\kappa|^2-|w_m|^2}{\bar{\omega}^2|n_m|^2}\right]\right]\times\frac{\pi\bar{\omega}^2 w_m^{-1}}{[w_m+i\,\mathrm{Im}(w_m)]}t_{mg}^p t_{gm}^p E_p^I|t_{gm}^s E_s^I|^2 , \tag{A3a}$$

$$\mathbf{E}_p^{RX}=-\hat{\mathbf{p}}_{g+}\left[A\left[\frac{\kappa^2-2w_m^2}{\bar{\omega}^2\epsilon_m}\right]-B\frac{w_m^2}{\bar{\omega}^2\epsilon_m}\right]\times\frac{\pi\bar{\omega}^2 w_m^{-1}}{[w_m+i\bar{\omega}\,\mathrm{Im}(n_m)]}t_{mg}^p t_{gm}^p E_p^I|t_{gm}^0 E_p^N|^2 . \tag{A3b}$$

The intensity reflectivity of specular reflection is defined by $R\equiv|\mathbf{E}_0^R|^2/|\mathbf{E}_0^I|^2$. Expressions for the nonlinear Fresnel reflection of the probe wave (to leading order) are given by

$$R_s=|r_{gm}^s|^2-\mathrm{Re}\left[\frac{4\pi^2(A+\frac{1}{2}B)}{cn_g\zeta[\zeta+i\,\mathrm{Im}(\zeta)]}r_{gm}^{s*}t_{mg}^s t_{gm}^s|t_{gm}^s|^2\right]I_{\mathrm{probe}}-\mathrm{Re}\left[\frac{8\pi^2(A+\frac{1}{2}B)}{cn_g\zeta[\zeta+i\,\mathrm{Im}(n_m)]}r_{gm}^{s*}t_{mg}^s t_{gm}^s|t_{gm}^0|^2\right]I_{\mathrm{pump}} \quad \text{(A4)}$$

for s-polarized probe and pump waves and by

$$R_p=|r_{gm}^p|^2-\mathrm{Re}\left[\frac{4\pi^2 U}{cn_g\zeta[\zeta+i\,\mathrm{Im}(\zeta)]}r_{gm}^{p*}t_{mg}^p t_{gm}^p|t_{gm}^p|^2\right]I_{\mathrm{probe}}-\mathrm{Re}\left[\frac{4\pi^2 V}{cn_g\zeta[\zeta+i\,\mathrm{Im}(n_m)]}r_{gm}^{p*}t_{mg}^p t_{gm}^p|t_{gm}^0|^2\right]I_{\mathrm{pump}} \quad \text{(A5)}$$

for p-polarized probe and pump waves, where

$$U=A(2\sin^2\theta_m-1)(|\sin\theta_m|^2+|\cos\theta_m|^2)+\tfrac{1}{2}B(|\sin\theta_m|^2-|\cos\theta_m|^2)\ , \quad \text{(A6a)}$$

$$V=A(3\sin^2\theta_m-2)-B\cos^2\theta_m\ , \quad \text{(A6b)}$$

the intensity of the probe wave in the material g is given by $I_{\mathrm{probe}}=(cn_g/2\pi)|\mathbf{E}^I|^2$ and $\zeta=n_m\cos\theta_m$.

*Also at Department of Physics, University of Rochester, Rochester, New York 14627.

[1] B. Ya Zel'dovich, N. F. Pilipetsky, and V. V. Shkunov, *Principles of Phase Conjugation* (Springer-Verlag, New York, 1985).

[2] O. L. Kulikov, N. F. Pilipetskii, A. N. Sudarkin, and V. V. Shkunov, Pis'ma Zh. Eksp. Teor. Fiz. **31**, 377 (1980) [JETP Lett. **31**, 345 (1980)].

[3] N. F. Pilipetskii, A. N. Sudarkin, V. V. Shkunov, and V. V. Yakimenko, Kvant. Elektron. (Moscow) **10**, 456 (1983) [Sov. J. Quantum Electron. **13**, 265 (1983)].

[4] A. A. Golubtsov, N. F. Pilipetskii, A. N. Sudarkin, and V. V. Shkunov, Kvant. Elektron. (Moscow) **8**, 663 (1981) [Sov. J. Quantum Electron. **11**, 402 (1981)].

[5] T. E. Zaporozhets and S. G. Odulov, Pis'ma Zh. Tekh. Fiz. **6**, 1391 (1980) [Sov. Tech. Phys. Lett. **6**, 599 (1980)].

[6] G. B. Al'tshuler, K. I. Krylov, V. A. Romanov, L. M. Studenikin, and V. Yu. Khramov, Pis'ma Zh. Tech. Fiz. **7**, 1458 (1981) [Sov. Tech. Phys. Lett. **7**, 624 (1981)].

[7] A. V. Mamaev, N. A. Melnikov, N. F. Pilipetsky, A. N. Sudarkin, and V. V. Shkunov, J. Opt. Soc. Am. A **1**, 856 (1984); Zh. Eksp. Teor. Fiz. **86**, 232 (1984) [Sov. Phys.—JETP **59**, 132 (1984].

[8] N. K. Berger, E. A. Zhukov, and V. V. Novokhatskii, Kvant. Elektron. (Moscow) **11**, 748 (1984) [Sov. J. Quantum Electron. **14**, 505 (1984)].

[9] A. E. Korolev, V. N. Nazarov, and D. I. Stasel'ko, Pis'ma Zh. Tekh. Fiz. **15**, 87 (1989) [Sov. Tech. Phys. Lett. **15**, 824 (1989)].

[10] O. V. Garibyan, I. N. Kompanets, A. V. Parfyonov, and N. F. Pilipetsky, V. V. Shkunov, A. N. Sudarkin, A. V. Sukhov, N. V. Tabiryan, A. A. Vasiliev, and B. Ya Zel'dovich, Opt. Commun. **38**, 67 (1981).

[11] J. M. Nunzi and D. Ricard, Appl. Phys. B **35**, 209 (1984).

[12] N. F. Pilipetskii, A. N. Sudarkin, and K. N. Ushakov, Zh. Eksp. Teor. Fiz. **93**, 118 (1987) [Sov. Phys. JETP **66**, 66 (1987)].

[13] B. Ya Zel'dovich, N. F. Pilipetskii, A. N. Sudarkin, and V. V. Shkunov, Dokl. Akad. Nauk SSR **252**, 92 (1980) [Sov. Phys. Dokl. **25**, 377 (1980)].

[14] K. Ujihara, Opt. Commun. **42**, 1 (1982); **43**, 225 (1982); J. Opt. Soc. Am. **73**, 610 (1983).

[15] G. V. Arutyunyan and G. P. Dzhotyan, Opt. Spectrosc. **63**, 338 (1987).

[16] J. E. Sipe, J. Opt. Soc. Am. B **4**, 481 (1987).

[17] E. Hecht, *Optics*, 2nd ed. (Addison-Wesley, Reading, MA, 1987), Sec. 4.3.2.

[18] P. D. Maker and R. W. Terhune, Phys. Rev. A **137**, 801 (1965).

[19] R. W. Boyd, *Nonlinear Optics* (Academic, New York, 1992), Sec. 4.2.

[20] J. J. Maki, M. S. Malcuit, J. E. Sipe, and R. W. Boyd, Phys. Rev. Lett. **67**, 972 (1991).

[21] H. A. Lorentz, *The Theory of Electrons*, 2nd ed. (Dover, New York, 1952), Sec. 117–136 and Note 54.

[22] N. Bloembergen, *Nonlinear Optics* (Benjamin, New York 1965); see also J. A. Armstrong, N. Bloembergen, J. Ducuing, and P. S. Pershan, Phys. Rev. **127**, 1918 (1962); D. Bedeaux and N. Bloembergen, Physica **69**, 57 (1973).

[23] E. L. Lewis, Phys. Rep. **58**, 1 (1980).

[24] W. L. Wiese, M. W. Smith, and B. M. Miles, *Atomic Transition Probabilities*, Natl. Bur. Stand. Ref. Data Ser., Natl. Bur. Stand. (U.S.) Circ. No. 22 (U.S. GPO, Washington, DC, 1969), Vol. 2.